Modeling GCM and scenario uncertainty using a possibilistic approach: Application to the Mahanadi River, India

P. P. Mujumdar[1] and Subimal Ghosh[2]

Received 24 April 2007; revised 20 October 2007; accepted 29 January 2008; published 11 June 2008.

[1] Climate change impact assessment on water resources with downscaled General Circulation Model (GCM) simulation output is characterized by uncertainty due to incomplete knowledge about the underlying geophysical processes of global change (GCM uncertainties) and due to uncertain future scenarios (scenario uncertainties). Disagreement between different GCMs and scenarios in regional climate change impact studies indicates that overreliance on a single GCM with a scenario could lead to inappropriate planning and adaptation responses. This paper focuses on modeling GCM and scenario uncertainty using possibility theory in projecting streamflow of Mahanadi river, at Hirakud, India. A downscaling method based on fuzzy clustering and Relevance Vector Machine (RVM) is applied to project monsoon streamflow from three GCMs with two green house emission scenarios. Possibilities are assigned to all the GCMs with scenarios based on their performance in modeling the streamflow of the recent past (1991–2005), when there are signals of climate forcing. The possibilities associated with different GCMs and scenarios are used as weights in computing the possibilistic mean of the CDFs projected for three standard time slices 2020s, 2050s, and 2080s. The result shows that the value of streamflow at which the CDF reaches 1 reduces with time, which shows the reduction in probability of occurrence of extreme high flow events in future. Historic record of monsoon streamflow of Mahanadi river also shows similar decreasing trend, which may be due to the effect of high surface warming. Reduction in Mahandai streamflow is likely to pose a major challenge for water resources engineers in meeting water demands in future.

Citation: Mujumdar, P. P., and S. Ghosh (2008), Modeling GCM and scenario uncertainty using a possibilistic approach: Application to the Mahanadi River, India, *Water Resour. Res.*, *44*, W06407, doi:10.1029/2007WR006137.

1. Introduction

[2] Climate change estimates on regional or local spatial scales are burdened with a considerable amount of uncertainty, stemming from several sources. *Huth* [2004] stated "For estimates based on downscaling of General Circulation Model (GCM) outputs, different levels of uncertainty are related to: (1) GCM uncertainty or intermodel variability, (2) scenario uncertainty or interscenario variability, (3) different realizations of a given GCM due to parameter uncertainty (intramodel variability) and (4) uncertainty due to downscaling methods". Uncertainty in initial conditions will also give rise to different GCM realizations. This paper focuses on the first two sources of uncertainties in assessment of climate change impact on streamflow and its application to the Mahanadi basin in India. GCM uncertainty, which is due to incomplete knowledge about the underlying geophysical processes of global change, coarse grid resolutions and unresolved processes leads to limitations in the accuracy of the models. Scenario uncertainty results from unpredictability in the forecast of future socioeconomic and human behavior resulting in future green house gas (GHG) emission scenarios. Downscaled outputs of a single GCM with a single climate change scenario represent a single trajectory among a number of realizations derived using various scenarios with GCMs. Such a single trajectory alone cannot represent a future hydrologic scenario, and will not be useful in assessing hydrologic impacts due to climate change. *Simonovic and Li* [2003, 2004] have shown the uncertainty lying in climate change impact studies on flood protection resulting from selection of GCMs and scenarios. Use of several GCMs and scenarios leads to a wide spread in the downscaled hydrologic projection, especially in years far into the future leading to uncertainties as to which among the several possible predictions should be used in developing responses.

[3] Research into probabilistic forecasts of climate change has been advancing rapidly on several fronts. *New and Hulme* [2000] developed a model for scenario uncertainty using Bayesian Monte-Carlo approach assuming a prior distribution of the uncertain parameters of the climate models. GCM uncertainty is presented in terms of sensitivity of climate change model outputs to streamflow. A similar methodology for sensitivity analysis and risk assessment of irrigation demand is given by *Jones* [2000].

[1]Department of Civil Engineering, Indian Institute of Science, Bangalore, India.
[2]Department of Civil Engineering, Indian Institute of Technology Bombay, Mumbai, India.

0043-1397/08/2007WR006137$09.00

Bayesian models have been applied by *Allen et al.* [2000] to multimodel ensembles to characterize uncertainty and the probability density function (pdf) of temperature for future climate changes at regional scales. *Giorgi and Mearns* [2003] developed a Reliability Ensemble Averaging (REA) method for estimating probability of regional climate change exceeding given thresholds based on ensembles of different model simulations. Weights are assigned to different GCMs based on their bias with respect to the observed data and the convergence of the simulated changes across models. Such a model is further modified in Bayesian framework by *Tebaldi et al.* [2004, 2005]. They developed a Bayesian approach to determine pdfs of temperature change at regional scales, from the output of a multimodel ensemble, run under the same scenario of future anthropogenic emissions. A simple probabilistic energy balance model, that samples uncertainty in greenhouse gas emissions, climate sensitivity, carbon cycle, ocean mixing, and aerosol forcing, is used by *Dessai et al.* [2005], to quantify uncertainty in regional climate change projections. Assignment of global mean temperature probabilities in GCMs through pattern scaling techniques has been suggested in that study. In order to combine the resulting probabilities, regional skill scores for each GCM, season, and climate variable (surface temperature, and precipitation) are devised in 23 world regions, based on model performance and model convergence. A range of sensitivity experiments is carried out with different skill score schemes, climate sensitivities, and emission scenarios for performing sensitivity analysis of regional climate change probabilities. *Wilby and Harris* [2006] developed a framework for assessing uncertainties in climate change impacts in projecting low flow scenarios of The Thames river, UK. A probabilistic framework is developed for combining information from an ensemble of four GCMs, two green house gas emission scenarios, two statistical downscaling techniques, two hydrologic model structures and two sets of hydrologic model parameters. GCMs are weighted based on the biases which are calculated with Impact Relevant Climate Prediction Index (IRCPI). The resulting CDFs derived from the downscaled projection are calculated with the impact to be most sensitive to the intermodel or GCM uncertainty. In all the models mentioned above, the bias in the GCM simulations is not corrected with respect to the observed period; rather, weights are assigned to the GCMs based on their individual bias. The GCM uncertainty modeled in those studies is due to the inherent bias present in the GCMs.

[4] *Ghosh and Mujumdar* [2007a] have used nonparametric methods in modeling GCM and scenario uncertainty for future drought assessment in Orissa meteorological subdivision, India. Samples of a drought indicator are generated with downscaled precipitation from available GCMs and scenarios. In that study the bias has been corrected for each GCM with respect to the observed data of baseline period (years 1961–1990) and it is assumed that bias free GCM simulations are equally accurate across all GCMs and all the scenarios are equally possible. With this assumption, nonparametric methods such as kernel density estimation and orthonormal series methods are used to determine the pdf of the drought indicator. Scenario uncertainty is considered in the model by incorporating simulations of different scenarios. The information generated through the pdf of the drought indicator in a future year, can be used in long term planning decisions. A limitation in the model is that all scenarios are not available under all GCMs, and therefore, outputs of some of the scenarios for a few GCMs are missing which may lead to partial ignorance. Moreover, the set of available scenarios may not fully compose the universal sample space, Ω, which is defined to contain all possible scenarios and thus precise or conventional probability is not expressive enough for application to scenarios [*Tonn*, 2005]. To model partial ignorance resulting from the above mentioned reasons, the methodology is further extended [*Ghosh and Mujumdar*, 2007b] with the concept of imprecise probability or interval probability. A normal distribution is assumed for the drought indicator for each year, with imprecision inherent in it. Uncertainty underlying in this assumption and that due to partial ignorance about future scenarios are modeled by fitting the normal distribution to drought indicator with interval regression leading to a imprecise normal distribution resulting in imprecise probabilities. In imprecise probability, probability is expressed as interval grey number, a number with known lower and upper bounds but unknown distribution information.

[5] Dissimilarities between the bias-corrected GCM simulations under different scenarios after the year 1990 (end of baseline period) result in different system performance measures which do not validate the assumptions of equipredictability of GCMs and equipossibility of scenarios, which are made in the analysis by *Ghosh and Mujumdar* [2007a, 2007b]. An evaluation of climate change impact, in terms of quantification of change in hydrologic and climatological variables is performed with respect to the baseline period 1961–1990 (http://sedac.ciesin.columbia.edu/ddc/baseline/index.html). Following this it is assumed in the present study that the impact of climate forcing will be visible after 1990, or in other words after 1990 the change in the climate and hydrologic variable will be quantified with respect to those of the baseline period. For appropriate planning and adaptation responses, with the passage of time, it is relevant to assess the effectiveness of the GCMs in best modeling climate change and also to judge which of the scenarios best represent the present situation under climate forcing. The objective of this study is to model the uncertainty in climate change derived from different GCMs and scenarios by assigning possibility distribution to different GCMs and scenarios, measured in terms of their ability in modeling climate change based on their performance in the recent past (years 1991–2005) under climate forcing. To do this, we use possibility theory, which is an uncertainty theory devoted to addressing partially inconsistent knowledge and linguistic information based on intuitions. Unlike probability, possibility is not computed from a frequency resulting from a sample, but is assigned to an event based on intuitive argumentation [*Spott*, 1999]. In the present study, such intuition about the future hydrologic condition, is derived based on the performance of GCMs with associated scenarios. On the basis of such intuition, a possibility mass function is derived with possibility values assigned to the GCMs and scenarios. ''possibility assigned to a GCM' is interpreted here as the possibility with which the future hydrologic variable of interest is modeled best

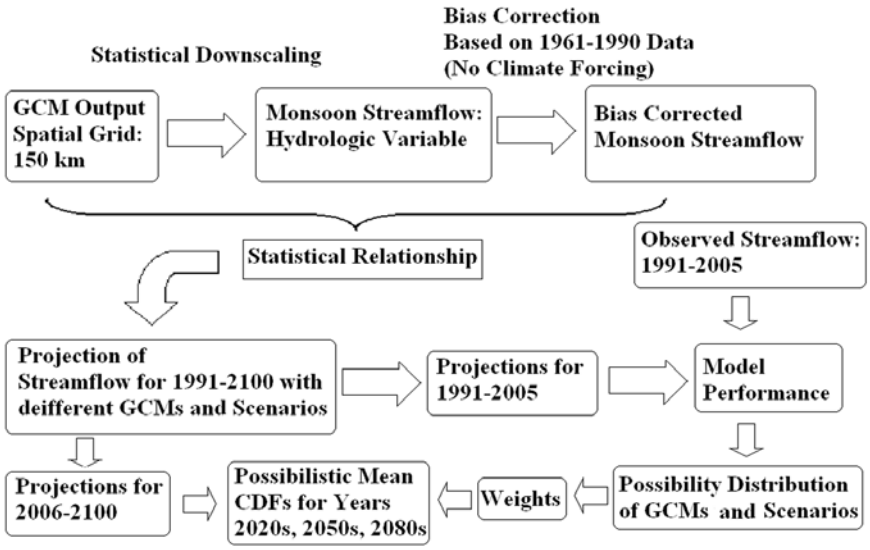

Figure 1. Overview of the possibility model.

by the downscaled output of the GCM. Similarly," possibility assigned to a scenario' denotes the possibility with which the scenario best represents the climate forcing resulting in the change in the hydrologic variable. The possibility values thus computed are used as weights in deriving a possibilistic mean CDF (weighted CDF) of future hydrologic variable for time slices 2020s (years 2006–2035), 2050s (years 2036–2065), and 2080s (years 2066–2095). The following section presents a brief overview on data used and the methodology used in the present study.

2. Data and Methods

[6] Figure 1 presents an overview of the possibilistic approach used in this paper in modeling GCM and scenario uncertainty. The approach typically involves statistical downscaling with bias correction and assignment of possibilities to all GCMs and scenarios based on performance during recent past. Application of the possibilistic model is demonstrated with the monsoon streamflow of Mahanadi at Hirakud dam. A statistical downscaling model based on PCA, fuzzy clustering and Relevance Vector Machine (RVM) is developed to predict the monsoon streamflow of Mahanadi river at Hirakud reservoir, from GCM projections of large scale climatological data. Surface air temperature at 2 m, Mean Sea Level Pressure (MSLP), geopotential height at a pressure level of 500 hecto Pascal (hPa) and surface specific humidity are considered as the predictors for modeling Mahanadi streamflow in monsoon season. Three GCMs, CCSR/NIES coupled model developed by Center for Climate System Research/National Institute for Environmental Studies (CCSR/NIES), Japan, Hadley Climate Model 3 (HadCM3), developed by Hadley Centre for Climate Prediction and Research, U.K. and Coupled Global Climate Model 2 (CGCM2), developed by Canadian Center for Climate Modeling and Analysis, Canada with two scenarios, A2 and B2 are used for the purpose. The simulation period of the models CCSR/NIES, HadCM3 and CGCM2 are 1890–2100, 1950–2100 and 1900–2100 respectively (http://www.mad.zmaw.de/IPCC/DDC/html/SRES/TAR/index.html). Possibilities are assigned to GCMs and scenarios based on their performances in predicting the streamflow during years 1991–2005, when signals of climate forcing are visible. The possibilities are used as weights for deriving the possibilistic mean CDF for the three standard time slices of 2020s, 2050s and 2080s. The following subsection presents the details of case–study are and the data used.

2.1. Study Area and Observed Streamflow Data

[7] The Mahanadi river of eastern India, rises on the Amarkantak plateau in the Eastern Ghats in central India in Chhatishgarh. It drains most of the state of Chhattisgarh, much of Orissa, and portions of Jharkhand and flows east to the Bay of Bengal. The data considered for this case-study are the inflow to the Hirakud dam, which is located on Mahanadi river in Orissa (21.32°N, 83.45°E) at east coast of India (Figure 2). The monthly inflow to Hirakud dam from 1961 to 2005, is obtained from the Department of Irrigation, Government of Orissa, India. Because of an absence of any major control structure upstream of the Hirakud reservoir, the inflow to the dam is considered as unregulated flow. The Mahanadi River is a rain-fed river with high streamflow during June to September due to monsoon rainfall, with insignificant contribution from groundwater during this season. In the nonmonsoon season, low rainfall results in low flow conditions, compared to which groundwater component is significant. Moreover, the monsoon flows are important in Hirakud reservoir to meet the demands during the year. Thus the monsoon streamflow is only modeled here using the atmospheric variables without considering groundwater component. The monthly monsoon flow data of Mahanadi at the Hirakud reservoir from year 1961 to year 2005 is used in the analysis. Figure 3 presents the monsoon flow of the Mahanadi River for the period 1961–2005. Box plots are plotted separately for the baseline periods (1961–1990) and the recent past (1991–2005). It shows a decrease in the streamflow in the recent past with

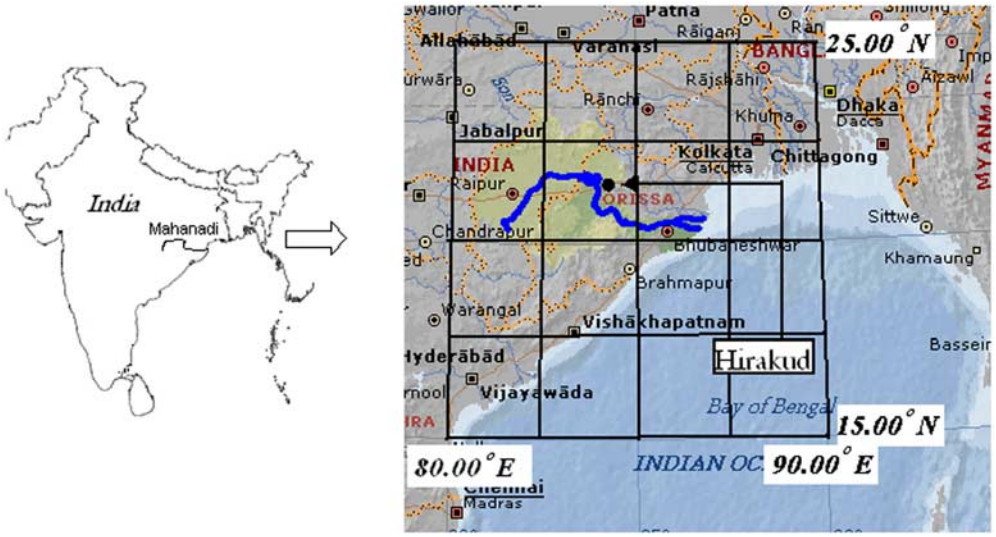

Figure 2. NCEP grids superposed on Mahanadi River basin.

respect to that of baseline period which can be considered as an impact of "climate signal."

2.2. Development of the Downscaling Model

[8] The statistical downscaling model [*Ghosh and Mujumdar*, 2008] used in present study consists of PCA, fuzzy clustering and relevance vector machine. Selection of the predictor is an important step in statistical downscaling. The predictors used for downscaling should be [*Wilby et al.*, 1999; *Wetterhall et al.*, 2005]: (1) reliably simulated by GCMs, (2) readily available from archives of GCM outputs, and (3) strongly correlated with the surface variables of interest. *Cannon and Whitfield* [2002] have used MSLP, 500 hPa geopotential height, 800 hPa specific humidity, and 100–500 hPa thickness field as the predictors for downscaling GCM output to streamflow. Monsoon streamflow can be considered broadly as a resultant of rainfall and evaporation. Rainfall is a consequence of Mean Sea Level Pressure (MSLP) [*Bardossy and Plate*, 1991; *Bardossy et al.*, 1995; *Hughes and Guttorp*, 1994; *Wetterhall et al.*, 2005], geopotential height and humidity whereas evaporation is mainly influenced by temperature and humidity. Therefore the present study considers 2m surface air temperature, MSLP, 500 hPa geopotential height and surface specific humidity as the predictors for modeling streamflow in the monsoon season. It is worth mentioning that land use is one of the important factors in generating the streamflow from rainfall because of the

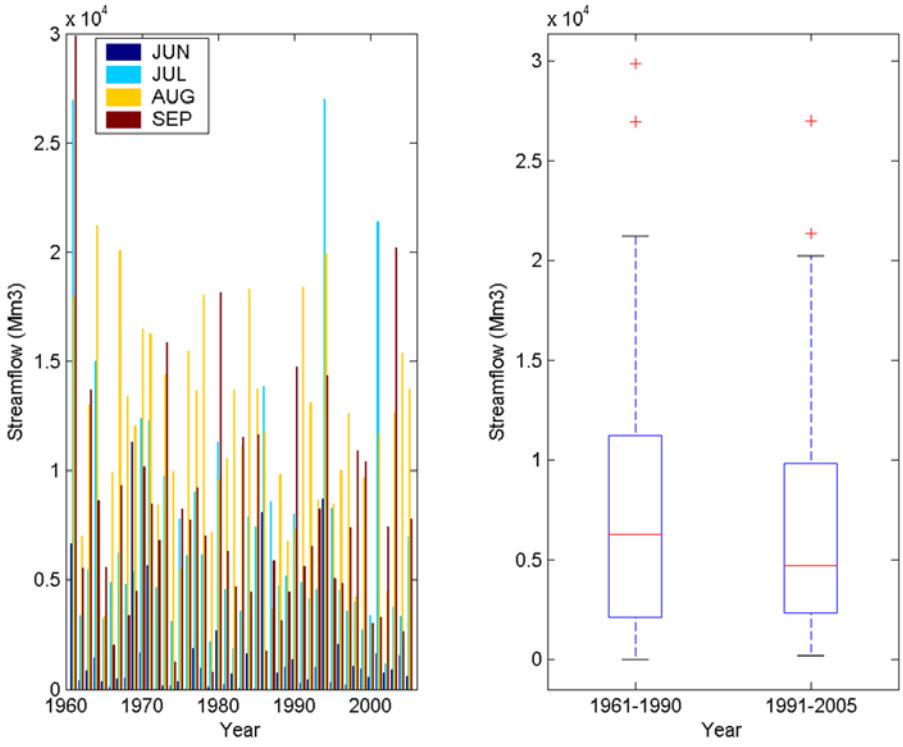

Figure 3. Monsoon streamflow of Mahanadi River at Hirakud.

impact of the land cover on runoff process [*Brath et al.*, 2006]. In the present study, land use pattern is assumed to remain the same in future and therefore the statistical relationship between the predictors and streamflow will remain unaltered in the future. Gridded values of predictors are obtained from the National Center for Environmental Prediction/National Center for Atmospheric Research (NCEP/NCAR) reanalysis project [*Kalnay et al.*, 1996; http://www.cdc.noaa.gov/cdc/reanalysis/reanalysis.shtml] in the absence of observed atmospheric data. Reanalysis data are outputs from a high resolution atmospheric model that has been run using data assimilated from surface observation stations, upper-air stations, and satellite-observing platforms. Results obtained using these fields therefore represent those that could be expected from an ideal GCM [*Cannon and Whitfield*, 2002]. Monthly climate data were obtained from the NCEP/NCAR reanalysis project for 1961 to 1990 for a region spanning $15°N - 25°N$ and $80°E - 90°E$. Figure 2 shows the NCEP grid points superposed on the map of the Mahanadi river basin.

[9] Monsoon streamflow at Hirakud in Mahanadi river is projected from the GCM output by statistical downscaling using Relevance Vector Machine (RVM) technique [*Ghosh and Mujumdar*, 2008]. The methodology involves Principal Component Analysis (PCA), fuzzy clustering and RVM. Standardization [*Wilby et al.*, 2004] is used prior to statistical downscaling to reduce systematic biases in the mean and variances of GCM predictors relative to the observations or NCEP/NCAR data. The procedure typically involves subtraction of mean and division by standard deviation of the predictor variable for a predefined base–line period for both NCEP/NCAR and GCM output. The period 1961–1990 is used as abase–line because it is of sufficient duration to establish a reliable climatology, yet not too long nor too contemporary to include a strong global change signal [*Wilby et al.*, 2004]. For the Mahanadi river basin, monthly values of four predictor variables (MSLP, 2m surface air temperature, specific humidity, and 500hPa geopotential height) over June, July, August and September at 25 NCEP grid points are used as predictors which are highly correlated in apace as well as with each other. With the 4 predictor variables at 25 NCEP grid points, Principal Component Analysis (PCA) is performed to convert them into a set of uncorrelated variables. It was found that 98.1% of the variability of the original data set is explained by the first 10 principal components and therefore only the first ten principal components are used for modeling streamflow. Fuzzy clustering is used to classify the principal components into classes or clusters assuming the existence of classes/clusters in climate variables and the relationship between the streamflow and climate variables are different for different clusters. It is observed by *Ghosh and Mujumdar* [2007a, 2008] that a heuristic classification of large scale GCM outputs based on fuzzy clustering, prior to regression, improves the model performance and thus in the present study RVM coupled with PCA and fuzzy clustering are used to downscale GCM output to streamflow. Fuzzy clustering assigns membership values of the classes to various data points, and it is more generalized and useful to describe a point not by a crisp cluster, but by its membership values in all the clusters [*Ross*, 1997]. The number of clusters is considered as 3, and the fuzzification parameter as 1.4 based on the Fuzziness Performance Index (FPI) and Normalized Classification Entropy (NCE) [*Güler and Thyne*, 2004]. The sum of the membership of a data point in 3 clusters is equal to 1 and thus the membership of only 2 clusters will automatically fix that of the other and are sufficient to be used as an input to the vector machine. Details of fuzzy clustering for downscaling are available by *Ghosh and Mujumdar* [2007a, 2008]. Thus the number of input variables used in the RVM is 12 (10 principal components and two memberships).

[10] RVM [*Tipping*, 2001] is a statistical tool which is capable of capturing nonlinear relationship between the predictors and predictand with minimum overfitting. The mathematical structure of an RVM model is similar to Support Vector Machine (SVM). Given a training data $\{(x_1,y_1),\ldots,(x_l,y_l),\ X \in \Re^n,\ Y \in \Re\}$, the RVM regression equation may be given by:

$$f(x) = \sum_{i=1}^{l} w_i \times K(x_i, x) + b \tag{1}$$

where, $K(x_i,\ x)$ and w_i are the kernel functions and the corresponding weights used in the RVM. b is a constant known as bias. The i^{th} input x_i for training is called Relevant Vector (RV) if $w_i \neq 0$ for that particular i. x is the input variable of the SVM. In equation (1) inputs other than support vectors vanish, after training. For the downscaling model developed in this chapter, x denotes set of principal components and cluster membership values, whereas, $f(x)$ denotes the streamflow. Bayesian analysis is used in an RVM to compute the relevant vectors along with the corresponding weights. Compared to SVM, RVM involves only a few relevant vectors from the training data set for regression and therefore reduces the possibility of overfitting. The choice of kernel function and its width is a major criterion in selection of appropriate RVM regression model. The RVM model is first trained and tested in K-fold cross validation (K = 10) with Gaussian, Laplacian and heavy-tailed Radial Basis Functions (RBFs), for a fixed value of kernel width (=1). In this procedure, the training set is partitioned into K disjoint sets. The model is trained, for a chosen kernel, on all the subsets except for one, which is left for testing. The procedure is repeated for a total of K trials, each time using a different subset for testing. The average of the R values obtained from all the K trials is considered as the R value for training. Similarly average of the R values obtained from testing of all the K disjoint sets is considered as the R value for testing. It is observed that heavy tailed RBF results maximum value of the correlations coefficient (R) between observed and predicted value for the testing data set showing minimum overfitting. After selecting the kernel function a sensitivity analysis is performed to see the effect of kernel width on training and testing R values. For kernel width 1.9, the testing R values reaches maximum (0.73) with a satisfactory training R value, 0.77, considering only 7.41% of the training data set as relevant vectors. Detailed description of the training and testing of RVM model is given by *Ghosh and Mujumdar* [2008]. After the selection of the kernel function and its width the whole data set is trained using RVM based regression with heavy-tailed RBF as the kernel. The R value is obtained as 0.82. After the calibration of the RVM regression model, it is used for modeling of future

streamflow time series from the predictor variables as projected by the GCMs under the A2 and B2 scenarios.

2.3. Prediction of Future Streamflow Using GCM Data

[11] The GCMs used in the present study are CCSR/NIES, Japan, HadCM3, U.K., and CGCM2, Canada and the scenarios are A2 and B2. Because of the unavailability of the predictor variables from other GCMs and scenarios (Third Assessment Report), the analysis is limited only to the three GCMs (CCSR/NIES, Japan; CGCM2, Canada; and HadCM3, U.K.) and the two scenarios (IPCC TAR scenarios A2 and B2). The GCM outputs are extracted from the IPCC data distribution center (http://www.mad.zmaw.de/IPCC_DDC/html/ddc_gcmdata.html), for the region covering all the NCEP grid points. For the baseline period 1961–1990, the A2 and B2 scenario runs are the same, as they are forced with the same 20th century forcing. The A2 storyline and scenario family describes a very heterogeneous world. The underlying theme is self-reliance and preservation of local identities. Fertility patterns across regions converge very slowly, which results in continuously increasing population. Economic development is primarily regionally oriented and per capita economic growth and technological change more fragmented and slower than other storylines. The B2 storyline and scenario family describes a world in which the emphasis is on local solutions to economic, social and environmental sustainability. It is a world with continuously increasing global population, at a rate lower than A2, intermediate levels of economic development, and less rapid and more diverse technological change. While the scenario is also oriented toward environmental protection and social equity, it focuses on local and regional levels. The expected increase in global temperature for the next century for scenarios A2 and B2 are nearly 3.4°C and 2.4°C [*IPCC*, 2001].

[12] GCM grid points do not match with NCEP grid points and thus interpolation is required to obtain the GCM output at NCEP grid points. Interpolation is performed with a linear inverse square procedure using spherical distances [*Willmott et al.*, 1985]. For example, for the GCM developed by CCSR/NIES, Japan, the grid size is 5.5° latitude × 5.625° longitude. The output is extracted for the Mahanadi river basin at 16 grid points extending from 13.8445°N to 30.4576°N and 78.7500°E to 95.6250°E. These values are then interpolated to the 25 NCEP grid points. Standardization is performed after interpolation, prior to downscaling. The eigenvectors or principal directions obtained from NCEP data are used as reference to convert the gridded standardized GCM output to the corresponding principal components. Cluster memberships are computed for GCM outputs using the cluster centers obtained from NCEP/NCAR reanalysis data. The statistical relationship based on RVM developed between climatological variables and streamflow is then applied to the principal components and cluster memberships to predict the inflow to Hirakud reservoir.

[13] It is observed by *Ghosh and Mujumdar* [2008] that even after standardization, the bias is not significantly reduced because the methodology may reduce the bias in the mean and variance of the predictor variable but it is much harder to accommodate the biases in large-scale patterns of atmospheric circulation in GCMs (e.g., shifts in the dominant storm track relative to observed data) or unrealistic intervariable relationships [*Wilby and Dawson*, 2004]. To remove such bias from a given downscaled output, for all the GCMs and scenarios, the following methodology [*Ghosh and Mujumdar*, 2008] is used, which is similar to the method used by *Wood et al.* [2002] for removing biases from the predictors.

[14] • CDFs are calculated for the downscaled GCM-generated and observed streamflow for the years 1961–1990 using Weibull's probability plotting position.

[15] • For a given value of GCM-generated streamflow (X_{GCM}), the value of the CDF (CDF_{GCM}) is computed.

[16] • The observed streamflow value is obtained from the observed CDF corresponding to CDF_{GCM}.

[17] • The GCM-generated streamflow is replaced by this observed value.

[18] • The CDFs of GCM-generated and observed streamflow, obtained for the years 1961–1990, act as reference, and based on these, the correction is applied to the streamflow values obtained from the GCM for future.

[19] The correction for bias involved here is based on equiprobability transformation. From the CDFs of GCM simulated variables and observed variables for baseline period 1961–1990, the rule for the transformation (bias correction with equiprobability transformation) is derived, and then used in the future hydrologic scenarios for computation of bias free estimates of the hydrologic variable of interest. It should be noted that the assumption in this methodology for bias correction is that the bias in GCMs remain same in future. After the bias corrections the GCM projections under A2 and B2 scenarios are used for modeling GCM and scenario uncertainty.

2.4. Modeling Uncertainty With Possibility Theory

2.4.1. Background to Uncertainty

[20] Modeling of GCM and scenario uncertainty necessitates use of a number of GCM outputs of different scenarios for risk based studies of future hydrologic extremes. One major assumption in modeling scenario uncertainty in most available literature [*Giorgi and Mearns*, 2003; *Wilby and Harris*, 2006; *Ghosh and Mujumdar*, 2007a, 2007b] is that all scenarios are equally likely. This assumption is necessary because of ignorance about climate forcing. It is argued here that the signals of climate forcing, following the IPCC definition of baseline period (http://sedac.ciesin.columbia.edu/ddc/baseline/index.html), would be visible because of global warming after the year 1990. For appropriate planning and adaptation responses, with the passage of time, it is relevant to assess the effectiveness of GCMs in modeling climate change and also to judge which of the scenarios represent the present situation best under climate forcing. A methodology based on possibility distributions is developed here to model GCM and scenario uncertainty with an objective of assignment of possibility values to GCMs and scenarios depending on their performance in modeling signals of climate forcing. As a prerequisite, a brief overview of possibility theory is given in the following subsection.

2.4.2. Possibility Theory

[21] Possibility theory, founded by *Zadeh* [1978], is an uncertain theory devoted to addressing incomplete information, and partially inconsistent knowledge [*Dubois*, 2006]. It is related to the theory of fuzzy sets as a fuzzy restriction

which acts as an elastic constraint on the values that may be assigned to a variable [*Zadeh*, 1978]. More specifically, if F is a fuzzy subset of a universe of discourse $\Omega = u$ which is characterized by its membership function μ_F, then a proposition of the form "$\boldsymbol{X}$ is $\boldsymbol{F}$", where $\boldsymbol{X}$ is a variable taking values in Ω, induces a possibility distribution Π_X which equates the possibility of $\boldsymbol{X}$ taking the value u to $\mu_F(u)$ - the compatibility of u with F. In this way, $\boldsymbol{X}$ becomes a fuzzy variable which is associated with possibility distribution Π_X in much the same way as a random variable is associated with a probability distribution [*Zadeh*, 1978]. A main feature of possibility that distinguishes it from probability is that it is mainly ordinal and is not related with frequency of experiments. If, $\boldsymbol{X}$ is a variable in the universe Ω, and it is not possible to estimate $\boldsymbol{X}$ precisely, then the possibility that $\boldsymbol{X}$ can take the value x (i.e., the degree of possibility of $\boldsymbol{X} = x$) can be mathematically defined as [*Spott*, 1999]:

$$\Pi_x(x) : \Omega \rightarrow [0, 1] \tag{2}$$

where, $\Pi_X(x) = 0$ denotes that $\boldsymbol{X} = x$ is impossible and $\Pi_X(x) = 1$ denotes $\boldsymbol{X} = x$ is possible without any restriction. $\boldsymbol{X}$ is called a possibilistic variable. $\Pi_X(x) = 1$, $\forall x \in \Omega$ is interpreted as complete ignorance about $\boldsymbol{X}$ (i.e., everything is possible). Learning more about the location of $\boldsymbol{X}$ means restricting the range of possible values of $\boldsymbol{X}$.

[22] A possibility system [*Drakopoulos*, 1995] is a triple $(\Omega, \mathcal{B}, \Pi)$ where Ω is the set of all possible outcomes, $\mathcal{B}$ is sigma-algebra on Ω and Π is a real valued function defined for each $A \in \mathcal{B}$ such that:

$$\Pi(\Phi) = 0 \tag{3}$$

$$\Pi(\Omega) = 1 \tag{4}$$

$$\Pi(\cup_i A_i) = \mathbf{sup}_i(\Pi(A_i)) \tag{5}$$

[23] The operator "sup" or supremum refers to maximum. In a possibility distribution $\Pi_X(x)$ there must be at least one $\tilde{x}$ such that $\Pi_X(\tilde{x}) = 1$. This property is called normalization [*Spott*, 1999].

2.4.3. Assignment of Possibilities to GCMs and Scenarios

[24] Complete ignorance about climate forcing will lead to assignment of equal possibility (i.e., $\Pi_X(x) = 1 \; \forall \; x$) to all the GCMs and scenarios, or in other words, it can be interpreted as there being no restriction in selecting the range of GCMs and scenarios and thus, all GCMs and scenarios are equally possible. With the data available only for the baseline period 1961–1990, i.e., with no evidence of the signals of climate forcing, all the GCMs and scenarios may be construed to have equal possibility, all equal to 1. In such cases, only the bounds of CDF will be of interest and all the CDFs generated from the GCMs with various scenarios will be in the interval of the bounds. Such interval probability is also referred to as imprecise probability. With time, using the growing evidence from signals of climate forcing it should be relevant to assign a possibility distribution to the GCMs and scenarios based on their performance in the period where climate change is visible.

[25] Performance measures for a prediction model are normally expressed as a function of the deviation of model predicted data from the observed data at a particular time. As Coupled atmosphere-ocean GCM simulations cannot capture the actual year to year variation their performance must be measured in terms of the long-term statistics, for example, as the deviation of the CDF of the projected streamflow from that of observations. In this study, a system performance measure similar to the Nash-Sutcliffe coefficient [*Nash and Sutcliffe*, 1970] is formulated. The objective is not to compute the resemblance of the two time series of observed and predicted streamflow, but to compute the goodness of fit between the two CDFs derived by the observed and predicted streamflow using Weibull's probability plotting position. The co-efficient (C) used as a performance measure is given by:

$$C = 1 - \frac{\Sigma_F \left(Q_{oF} - Q_{pF}\right)^2}{\Sigma_F \left(Q_{oF} - \overline{Q_o}\right)^2} \tag{6}$$

where, Q_{oF} and Q_{pF} are the observed and predicted streamflow (by a GCM under a scenario) corresponding to a CDF value F, and $\overline{Q_o}$ is the mean observed streamflow. For computing C the CDF is divided into a discrete number of intervals and the quantiles are interpolated at those intervals (of size 0.05). Like the Nash-Sutcliffe coefficient, C can vary from 0 (when the model is linear and unbiased) to 1 with 0 indicating that the GCM fails to model the variability and predicts no better than the average of the observed data, and 1 indicating a perfect fit of the CDFs. The deviation of CDF of predicted variable from that of observed variable can also be computed using standard Kolmogorov-Smirnoff test, but to capture the essence of Nash-Sutcliffe coefficient (recommended by ASCE Task Committee on definition of Criteria for Evaluation of Watershed Models of the Watershed Management Committee, Irrigation and Drainage Division [1993]) the measure presented in equation (6) is used. It should be noted that C is computed only for the recent past (years 1991–2005). Being a measure of how well a particular scenario simulated by a GCM predicts the observed values during recent past, the coefficient C provides a measure of possibility value. As it is quite reasonable to expect that the CDF generated by a GCM will not perfectly match the observed CDF, a C value of 1 is nearly impossible. Therefore the results obtained from equation (6) cannot be used directly as the possibility for a particular GCM and scenario, because according to the properties of possibility distribution there should be at least one scenario simulated by any of the GCMs with a possibility value 1. To satisfy the property, the results obtained from equation (6) for all the three GCMs and associated scenarios, are normalized by dividing the C values with the maximum value of C and the normalized value thus obtained is used as the corresponding possibility value.

3. Results and Discussion

3.1. Predicted Streamflow for 1961–1990 Using Reanalysis Data

[26] The observed and predicted (from RVM) monsoon streamflow from June 1961 to August 1990, along with the scatterplot are presented in Figure 4. *Wetterhall et al.* [2005]

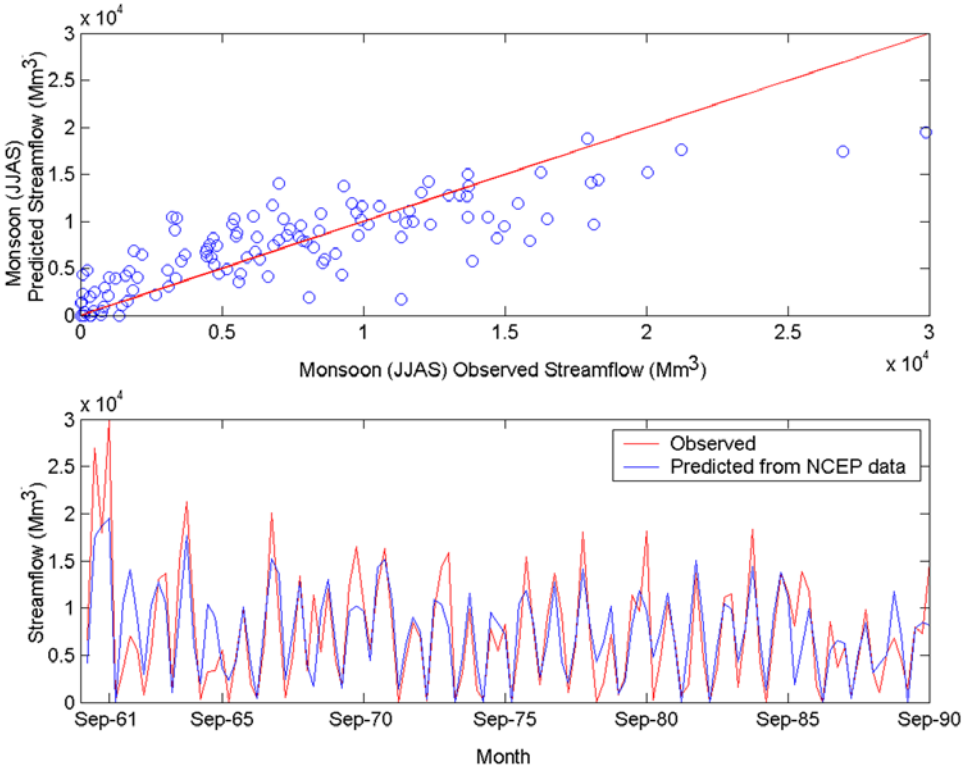

Figure 4. Observed and predicted streamflow (JJAS) of Mahanadi River.

have tested the long term seasonal mean, and standard deviation for verification of a downscaling model. In the present analysis a similar test was performed. The long term mean and standard deviation of observed streamflow are 7332.0 Mm^3 and 5995.6 Mm^3 and those of predicted streamflow are 7384.1 Mm^3 and 4607.6 Mm^3, which shows an acceptable match in central tendency (mean) but a significant difference in standard deviation. RVM based downscaling underestimates the observed high flows. One reason for this could be that the regression based statistical downscaling models often cannot explain the entire variance of the observed variable [*Wilby and Dawson*, 2004; *Tripathi et al.*, 2006]. The bias which is generally observed in the hydrologic variable downscaled with GCM outputs is the sum of the bias present in the downscaling model (in the RVM based statistical relationship) and in the GCM output. Both of them is adjusted at the end of downscaling using CDF matching approach (subsection 2.3).

3.2. Predicted Streamflow Using GCM Data

[27] The calibrated RVM model developed with reanalysis data is used to predict streamflow from the outputs of GCMs CCSR/NIES, CGCM2 and CSIRO-MK2 under A2 and B2 scenario. For validation of the downscaled GCM projections, the CDF obtained using Weibulls's plotting position for the baseline period (1961–1990) with the downscaled GCM projections is plotted with that of observed streamflow (Figure 5). In Figure 5, CDFs of the downscaled variable derived from different GCM outputs have significant deviations from that of the observed data which suggests that bias is not completely corrected using standardization and in such a condition, if the bias is not removed, the resulting uncertainty in future will not be solely due to modeled climate change but also due to the biases present in the GCMs. The bias is removed using the methodology of equiprobability transformation presented in subsection 2.3. The bias corrected streamflow projections with their corresponding CDFs for four time slices, 1991–2005, 2020s, 2050s and 2080s are presented in Figure 6. The figure shows that the CDF of streamflow downscaled from one GCM is entirely different from that of another and also that dissimilarity exists among two scenarios of any particular GCM although all scenarios project a reduction in monsoon flow. Another interesting feature in Figure 6 is the increased dissimilarity between the GCMs with time. The amount of uncertainty in 2080s is higher than those of the other time slices. This may point to different climate sensitivity among the models due to ignorance about the underlying geophysical processes. Such ignorance is addressed here with possibility theory [*Zadeh*, 1978; *Dubois*, 2006].

3.3. Possibilistic Modeling Results

[28] The performance measure C is computed for the 3 GCMs under A2 and B2 scenarios based on their prediction in the recent period (years 1991–2005). Values of C (unnormalized) for the three GCMs and the two scenarios are given in Table 1. The possibility distribution (or more appropriately, possibility mass function) obtained for the GCMs and scenarios (normalized values) is presented in Figure 7a. The difference between the possibility values of two GCMs for a given scenario is higher than that between the possibility values for two scenarios of a given GCM, which denotes that the uncertainty due to selection of GCM is greater than scenario uncertainty. The difference between the possibilities of the scenarios (A2 and B2) is highest for the GCM CCSR/NIES. The GCM, CGCM2 under A2 scenario has maximum

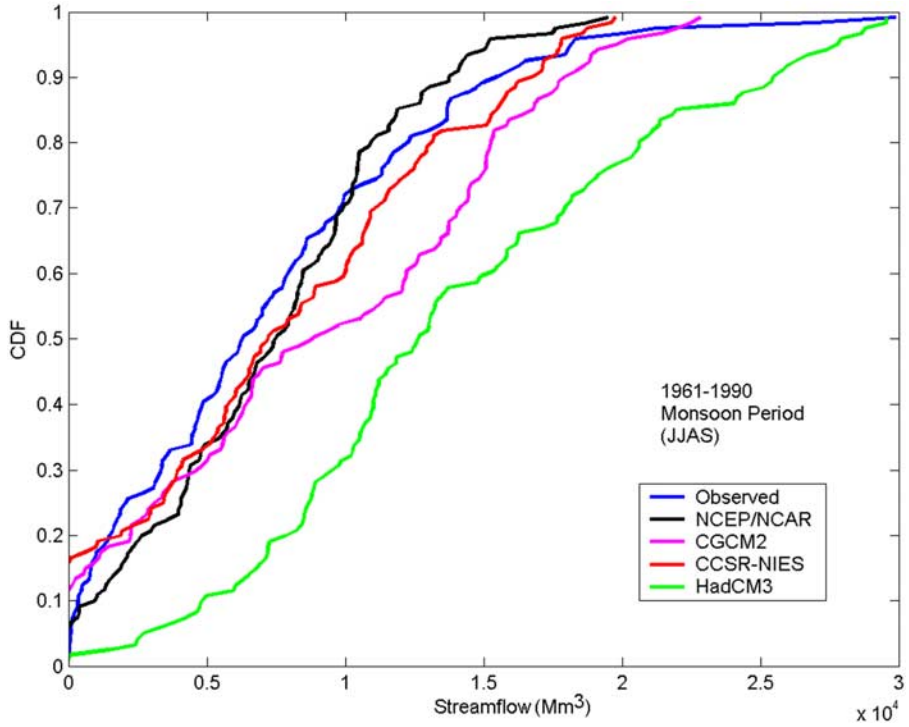

Figure 5. CDF of downscaled GCM projected streamflow for Baseline Period (1961–1990).

possibility whereas CCSR/NIES GCM under B2 scenario has minimum possibility. For the GCMs, CCSR/NIES and CGCM2, the C-score is higher for A2 scenario compared to B2 whereas, for the GCM HadCM3, B2 performs better than A2. This points to the dissimilarity of the projections simulated by different climate models. It is worth mentioning that a large difference is not observed between the possibilities for any two cases considered. This is because of the fact that the signal of climate forcing is not very pronounced in the initial time period (1991–2005) and therefore the results obtained by modeling climate forcing by GCMs are not significantly different from each other. With the passage of time, and with a stronger signal of climate change the possibility distribution information will

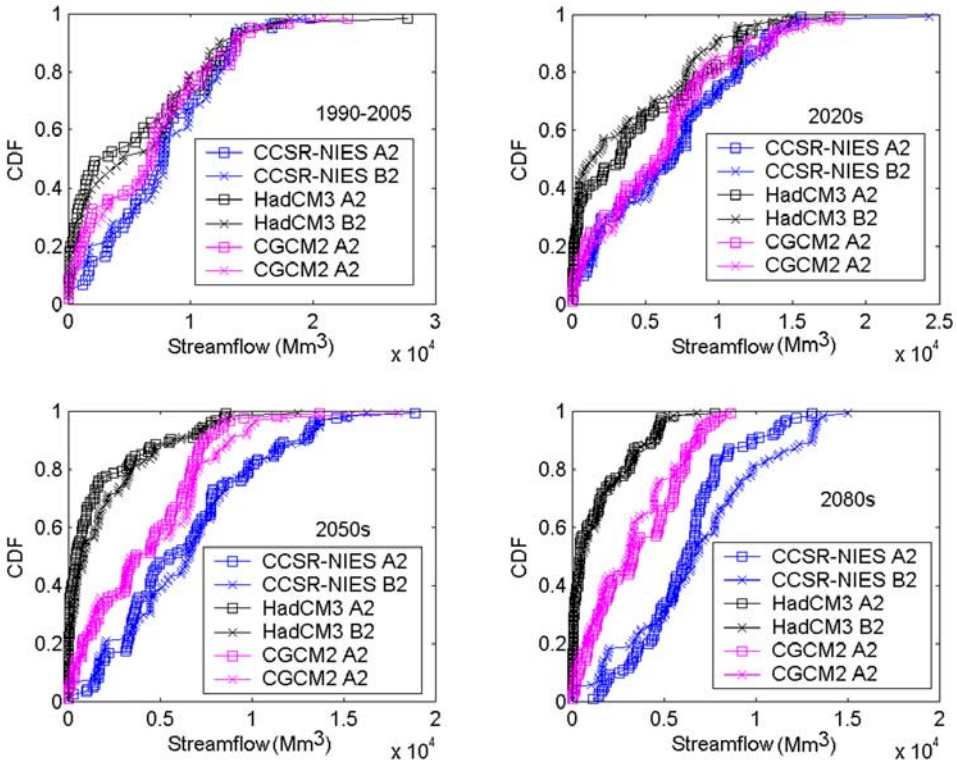

Figure 6. CDFs of bias corrected streamflow projections.

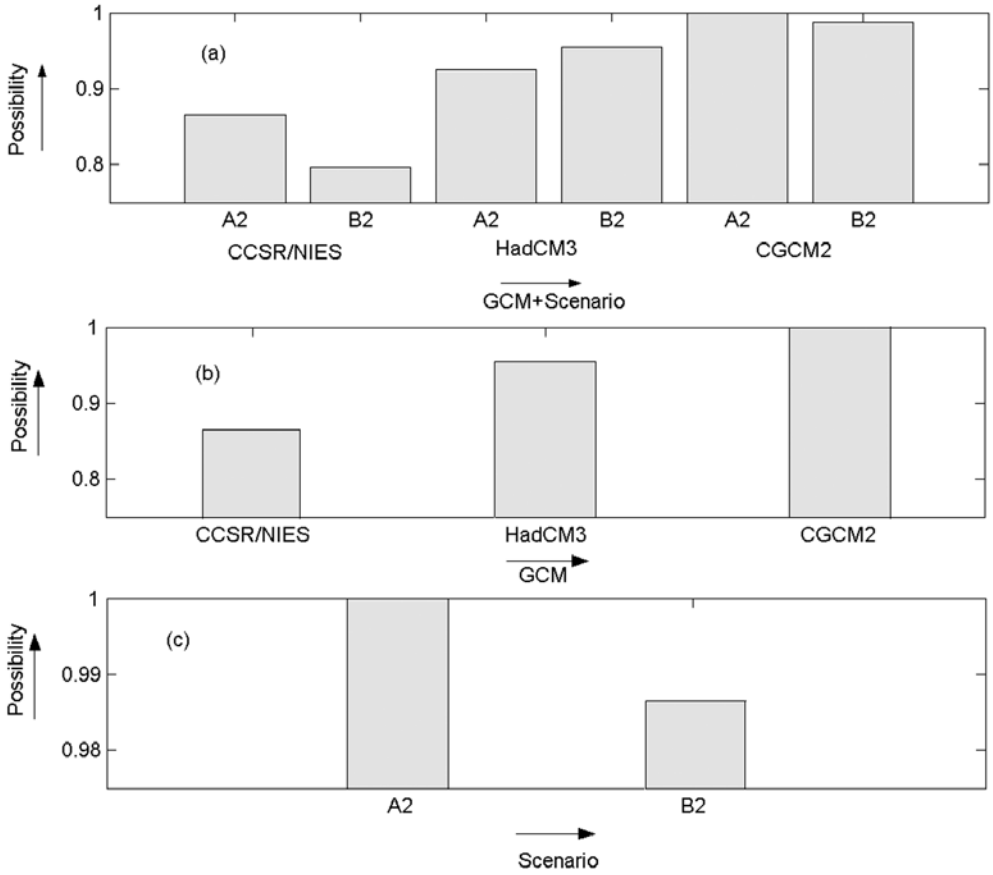

Figure 7. (a) Possibility distribution of GCMs and scenarios, (b) possibility distribution of GCMs, (c) possibility distribution of scenarios.

be more useful in assessing which of the GCMs is able to model the climate change the best and which of the scenarios the regional or local climate is actually following. This information, however is conditional on the downscaling method used and a change in downscaling model may change the resultant possibility distribution.

[29] Using the axioms of possibility distribution given in equations (3) to (5) the possibility distributions of the GCMs and scenarios are computed separately. For example, the possibility of GCM CCSR/NIES is given by:

$$\Pi(CCSR/NIES) = \Pi((CCSR/NIES, A2) \cup (CCSR/NIES, B2)) \tag{7}$$

$$= \mathbf{sup}(\Pi(CCSR/NIES, A2), \Pi(CCSR/NIES, B2)) \tag{8}$$

Similarly the possibility of a scenario (say A2) is given by:

$$\Pi(A2) = \Pi((CCSR/NIES, A2) \cup (HadCM3, A2) \cup (CGCM2, A2)) \tag{9}$$

$$= \mathbf{sup}(\Pi(CCSR/NIES, A2), \Pi(HadCM3, A2), \Pi(CGCM2, A2)) \tag{10}$$

[30] The possibility distributions of GCMs and scenarios are plotted separately in Figures 7b and 7c, which show CGCM2 to be the GCM having highest possibility value with A2 as the most possible scenario for use in regional climate change impact assessment for streamflow in the Mahanadi river basin. It should be noted that projection of a hydrologic variable other than streamflow may result in a different possibility distribution for the same region. A GCM/scenario with a possibility 1 does not imply that the particular GCM/scenario perfectly projects climate change, but in this case, it points to an ignorance of existence of any better GCMs or scenarios in modeling climate change impact on streamflow at the river basin scale. The possibility values obtained for each GCM and scenario are used as weights to compute the possibilistic mean CDF (F_{pm}) for the time slices 1991–2005, 2020s, 2050s, and 2080s.

$$F_{pm} = \frac{\Sigma_g \Sigma_s \Pi(g,s) \times F_{gs}}{\Sigma_g \Sigma_s \Pi(g,s)} \tag{11}$$

Table 1. Performance Measure C for the Three GCMs and the Two Scenarios

GCM	Scenario	C
CCSR/NIES	A2	0.8178
	B2	0.7533
HadCM3	A2	0.8743
	B2	0.9024
CGCM2	A2	0.9454
	B2	0.9327

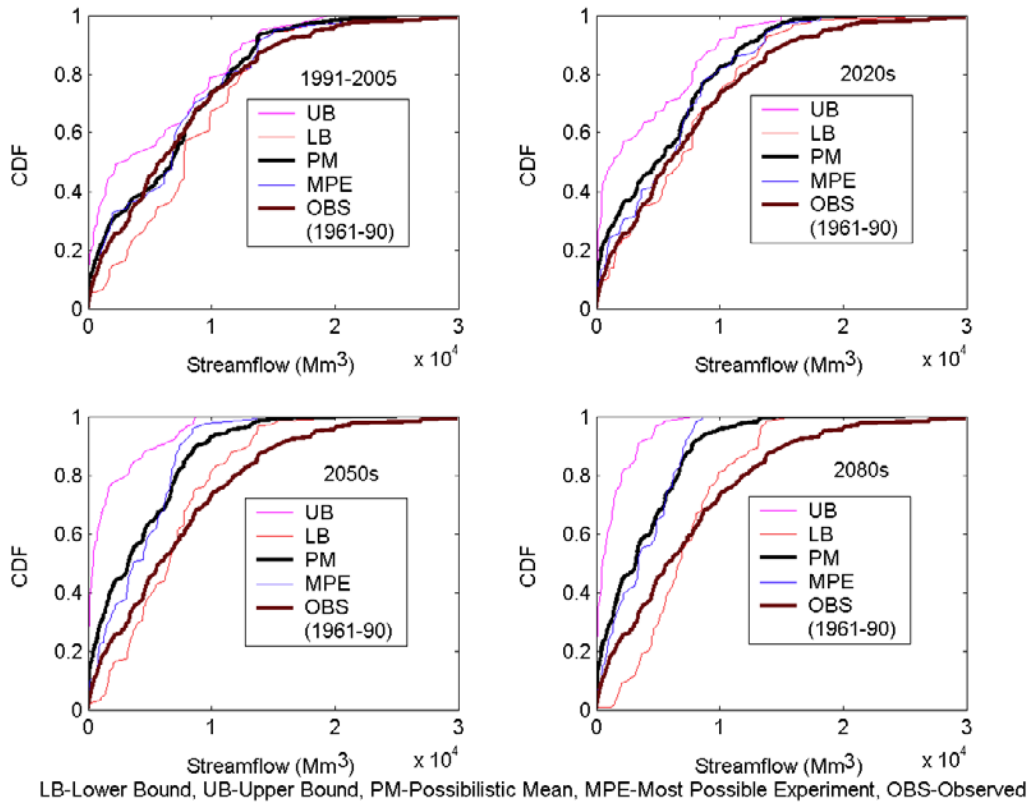

Figure 8. Upper bound, lower bound and possibilistic mean CDF.

where, $\Pi(g, s)$ and F_{gs} are the possibility and CDF associated with g^{th} GCM and s^{th} scenario. We also calculate the range in predictions from the GCM/scenario combinations to compare with the possibilistic mean CDF as follows. For each of the discrete streamflow values at equal intervals, maximum and minimum CDF values are obtained from the CDFs generated using the projections with three GCMs and two scenarios. The maximum and minimum CDF values are considered as upper and lower bounds of the CDF ($[F^+, F^-]$), resulting in an imprecise CDF. The interval between F^+ and F^- is known as the probability box. Without any information regarding signals of climate forcing, i.e., in absence of observed streamflow for years 1991–2005, ($[F^+, F^-]$) represents the band of imprecise CDF within which, all the CDFs generated by various GCMs and scenarios have equal possibility (all equal to 1) signifying complete ignorance about climate forcing and future scenarios. The upper and lower bounds, possibilistic mean CDF and the most possible CDF (CDF for the GCM/scenario with possibility 1) are presented in Figure 8 for years 1991–2005, 2020s, 2050s and 2080s. It is observed that the value of streamflow at which the possibilistic mean CDF reaches the value of 1 for years 2020s, 2050s and 2080s are lower than that of baseline period 1961–1990 and also reduces with time, which shows reduction in probability of occurrence of extreme high flow events in future and therefore there is likely to be a decreasing trend in the monthly peak flow. A discussion on these results is presented in the following subsection.

3.4. Discussion

[31] Table 2 presents the values of streamflow derived from the upper bound CDF, lower bound CDF and the difference between them corresponding to the CDF values of 0.25, 0.5, 0.75, 0.9, and 0.95, for the periods 2020s, 2050s, and 2080s. The computed difference quantifies the uncertainty associated with the assessment of hydrologic impacts of climate change. The results clearly show that for a given CDF value the amount of uncertainty increases with time, which may be due to different climate sensitivity among the models. Such an uncertainty points that the use of single GCM and single scenario is misleading in climate change impact studies. Therefore there is a need to use multimodel ensembles for prediction of hydrologic variables incorporating impact of climate change.

[32] Forecasts of hydrologic variable incorporating the impact of climate change are particularly useful when the forecasts are used in decision making. In explicit stochastic optimization models for decision making the predicted multimodel ensembles are difficult to use; rather a single CDF is required as an input to the optimization model. Multiple CDFs derived with different GCMs and scenarios are therefore not useful in decision making and an appropriate aggregation of the ensembles resulting in a single CDF is desirable. The possibilistic mean CDF is a resultant of all the CDFs derived with different GCMs and scenarios with their associated weights. It should be noted that an arithmetic mean CDF may also serve the same purpose but it assigns equal weights to all the GCMs and the scenarios.

Table 2. Uncertainty in Streamflow Projections

	Quantile [Streamflow, (Mm^3)]								
	2020s			2050s			2080s		
CDF value	UB CDF	LB CDF	Difference	UB CDF	LB CDF	Difference	UB CDF	LB CDF	Difference
0.25	131	2732	2601	63	3524	3461	76	4508	4433
0.50	1381	6807	5426	393	6576	6183	491	6690	6199
0.75	7329	10144	2815	1639	8623	6984	1638	9120	7482
0.90	9811	13412	3601	5584	13009	7425	3375	13070	9695
0.95	11313	15482	4169	7395	13667	6272	4675	13263	8586

The advantage of using possibilistic mean CDF over arithmetic mean CDF is that the possibilistic mean CDF assigns weights to GCMs and scenarios based on their performances in recent years under climate forcing. Most possible CDF (i.e., CDF with the highest possibility value) is also another option to be used in decision making, but this does not consider the projections derived with other GCMs and scenarios and at the same time it is also not guaranteed that the GCM under a scenario which performs best in the recent past of fifteen years will always perform better than other GCMs in future. In the present study, assignment of weights based on performance, resembles the Bayesian approach developed by *Tebaldi et al.* [2004, 2005]. The differences between the two approaches are: (1) Bayesian model assigns weights to GCMs based on the bias in their simulations for baseline period, whereas the possibilistic model corrects for the bias in GCM simulations and assigns weights based on their performance in the recent past after the baseline period when the signals of climate forcing are visible, and (2) Bayesian approach does not assign weights to scenarios and considers equal possibilities of scenarios, whereas the present model assigns different possibility values to different scenarios.

[33] Table 3 presents the values of streamflow corresponding to possibilistic mean CDF values of 0.25, 0.5, 0.75 and 0.9 for the periods 2020s, 2050s and 2080s. The results show that the monsoon flow of Mahanadi River is likely to reduce in future. The reduction of the flow is quantified with respect to the observed flow of baseline period 1961–1990. Significant changes are observed in the low flow conditions for the periods 2020s, 2050s and 2080s. For the high flow condition (flow corresponding to the CDF value of 0.95) the change is most significant for the period 2080s. An earlier study [*Rao*, 1995] on Mahanadi River also observed a decrease in monsoon streamflow for the historic period. One possible reason for such a decreasing trend reported in that study is the significant increase in temperature due to climate warming. Analysis of instrumental climate data has revealed that the mean surface temperature over India has increased at a rate of about 0.4°C per century [*Rao*, 1995], which is statistically significant. The increasing trend of temperature in the Mahanadi river basin due to climate change is even more severe. *Rao and Kumar* [1992] have found that the surface air temperature over this basin is increasing at a rate of 1.1°C per century, which is more than double the rate of increase for entire India. In the present study, the effects of the possible changes in predictor variables MSLP, geopotential height at 500hPa, surface specific humidity and surface temperature on the streamflow are analyzed individually and are presented in Figure 9 for the most possible experiment, CGCM2 under A2 scenario. Significant change is not observed in streamflow due to the change of MSLP. Also there is no significant trend in the time series of MSLP simulated by the GCM for the Mahanadi basin. The correlations of streamflow with temperature and geopotential height are negative whereas it has a positive correlation with specific humidity. The time series plots of temperature, specific humidity and geopotential height have a high increasing trend. Therefore the effect of temperature and geopotential height are negative and the effect of specific humidity is positive toward the change in monsoon streamflow of Mahanadi river. Details of the analysis are tabulated in Table 4 with the change in the average values of predictor variables in 2080s with respect to that of baseline period. It is observed that the summation of individual effects of the predictor variables results in a net decrease in streamflow which is also reflected in Figure 8 and Table 3. It should be noted that the analysis presented in Table 4 presents approximate change in streamflow and the possible reasons behind such change. As the correlation between the predictor variables is not considered in Table 4 and also the average of the predictors over all the GCM grid points on Mahanadi basin is considered without accounting for them individually, this analysis cannot give the accurate estimates. It is however helpful in pointing out the possible reasons of decrease in streamflow. The analysis suggests that increases in temperature and geopotential height are possible reasons for decrease in streamflow. With the increase of surface temperature, the specific humidity increases but such an increase in humidity is not sufficient to nullify the effect of change in the other predictor variables. In a recent study for the same region (Orissa meteorological subdivision), *Ghosh and Mujumdar* [2007a, 2007b] have also found an increasing trend of extreme meteorological drought which resembles the trend in projections of Mahanadi streamflow in the present study. Simultaneous occurrence of reduction in Mahanadi streamflow and increase in extreme drought pose a major challenge for water resources engineers in meeting water demands in future.

[34] The results presented in this paper are obtained for the RVM based downscaling model and it should be noted that a change in the downscaling technique may alter the results. Use of multiple downscaling techniques in modeling downscaling uncertainty should therefore be incorporated in assessment of hydrologic impacts of climate change. A limitation of the work presented here is that the methodology does not consider the uncertainty due to the use of multiple downscaling models. Another limitation of the model is that the Third Assessment Report (TAR)

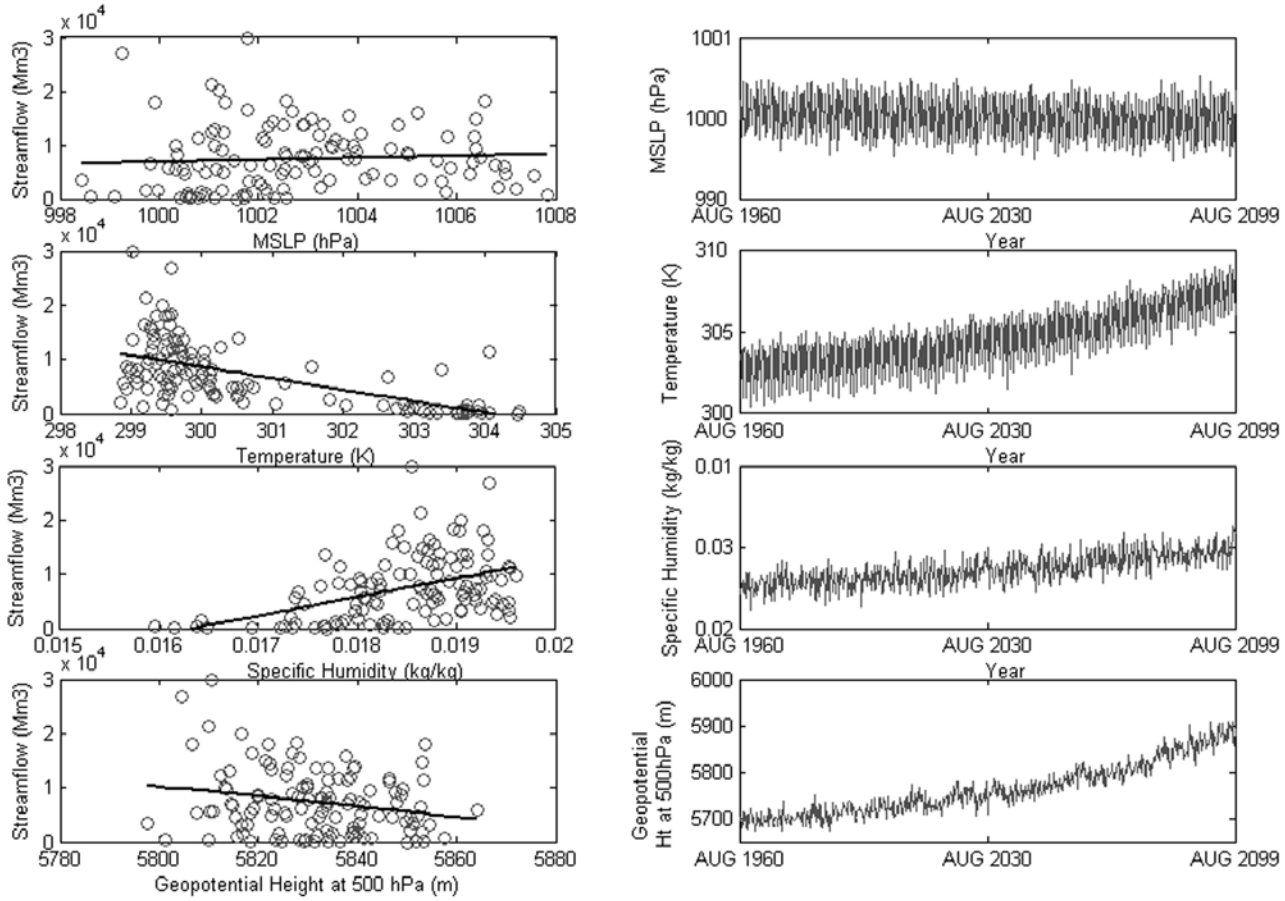

Figure 9. Effect of variations in predictor variables on Mahanadi streamflow.

data have been used in the present study which have very recently been replaced by Assessment Report 4 (AR4) data. Use of AR4 data involves substantially larger multimodel ensembles (of 17 GCMs) which may result in a more credible outcome. The difference between the possibility values for different GCMs and scenarios is very low because of the low dissimilarity between the projections simulated by different climate models for the validation period 1991–2005. Therefore the possibilistic mean CDF derived with the observed data of the validation period 1991–2005, may be similar to the arithmetic mean CDF. With the increase of the duration of validation period in future, the difference between the possibility values is also likely to increase with the increase of dissimilarities between the projections. In such a situation the results of possibilistic model will be more useful compared to those with the arithmetic mean CDF, in assessing which of the GCMs is able to model the climate change the best and which of the scenarios the regional or local climate is actually following. Although a significant difference between the projections simulated by different GCMs for a given scenario is observed, the difference between the projections under different scenarios is not significant for a given GCM. It should be noted that if the scenarios used in possibilistic model were very different for the period 1991–2005 and one scenario was more possible than the other, then the possibilistic mean CDF would be similar to the CDF generated by the GCM with maximum possibility with the most likely scenario. Insignificant differences between the projections under different scenarios for a given GCM may be because of the fact that, the greenhouse gas concentrations already in the atmosphere will impact the climate over the next few decades irrespective of future scenarios, and it is likely that the two scenarios A2 and B2

Table 3. Streamflow (in Mm^3) Derived From Possibilistic Mean CDF for Years 2020s, 2050s and 2080s

	1961–1990	2020s		2050s		2080s	
CDF Value	Streamflow	Streamflow	Change[a]	Streamflow	Change[a]	Streamflow	Change[a]
0.25	2063	911	−55.84%	774	−62.48%	791	−61.66%
0.50	6283	4926	−21.60%	3254	−48.21%	3180	−49.39%
0.75	11273	8480	−24.78%	6757	−40.06%	6018	−46.61%
0.90	15430	12170	−21.28%	8800	−27.69%	7788	−36.01%
0.95	18148	13773	−24.11%	11350	−37.46%	9725	−46.41%

[a]Change is measured with respect to the streamflow (Col.2) derived from the CDF of observed flow for the period 1961–1990.

Table 4. Effects of the Change in Predictor Variables on Streamflow

Predictors			Change in Streamflow, Mm^3	
GCM Simulated (1)	1961–1990 Average (2)	2080s Average (3)	Due to Unit Change in Predictor Variable (4)	Due to Total Change (Col3-Col2) in Predictor Variable
MSLP (hpa)	1000.82	999.6	186.49	−227.52
Temperature (K)	303.14	306.63	−2103.00	−7339.47
Specific humidity (kg/kg)	0.0156	0.0190	3.44×10^6	11696.00
Geopotential height (m)	5801.06	5869.22	−93.71	−6387.27
Total change in streamflow				−2258.26

will not diverge for many decades. Therefore significant difference between the possibilities assigned to different scenarios may not be observed in near future but there will be a growing difference between the possibility values assigned to GCMs with passage of time. Such a growing difference of the possibility values for different GCMs will increase the importance of the possibilistic model with time in future.

4. Concluding Remarks

[35] A methodology for modeling GCM and scenario uncertainty in a possibilistic framework is presented in this paper. Fuzzy clustering and RVM are used to downscale GCM output for projecting monsoon streamflow. Appropriate methodology is used to remove biases present in the GCMs based on observed data during baseline period (1961–1990) and therefore the bias free GCM projections present the uncertainty due to modeled climate change and not due to inherent bias. For water resources management it is important to know the effectiveness of the GCMs in modeling climate change and which of the scenarios best represent the present situation under global warming. Possibilities are assigned to GCMs and scenarios based on their system performance measure in predicting the streamflow during years 1991–2005, when signals of climate forcing are visible. Possibilities are further used as weights for deriving the possibilistic mean CDF for the three standard time slices 2020s, 2050s, and 2080s. A decreasing trend in future monsoon streamflow is predicted which may be the effect of high surface warming. It should be noted that till date the GCMs focus only on natural systems, and do not include socio-economic systems that affect and are affected by natural systems [*Simonovic and Davies*, 2006]. Natural and socioeconomic systems exhibit complex, nonlinear behavior, and affects each other, but conventionally they are treated as essentially independent. Consideration of socio-economic system and their interaction and feedback to natural systems (e.g., system dynamics approach) can provide more reliable projections of climatic and hydrologic variables in future. A limitation of the study presented in this paper is that uncertainties due to downscaling methods used are not addressed in the methodology. The study uses an RVM based downscaling technique, change of which may result in a different outcome. Incorporation of such uncertainty, without relying on a single downscaling technique may result in a more robust model for assessing hydrologic impacts of climate change.

[36] **Acknowledgments.** The authors sincerely thank two anonymous reviewers and the associate editor Alberto Montanari for reviewing the manuscript and providing critical comments to improve the paper. The work presented in this paper was financially supported by Indian National Committee on Hydrology (INCOH), Ministry of Water Resources, Govt. of India, through the research project 23/52/2006-R and D.

References

Allen, M. R., P. A. Stott, J. F. B. Mitchell, R. Schnur, and T. L. Delworth (2000), Quantifying the uncertainty in forecasts of anthropogenic climate change, *Nature*, *407*, 617–620.

Bardossy, A., and E. J. Plate (1991), Modeling daily rainfall using a semi-Markov representation of circulation pattern occurrence, *J. Hydrol.*, *122*, 33–47.

Bardossy, A., L. Duckstein, and I. Bogardi (1995), Fuzzy rule-based classification of atmospheric circulation patterns, *Int. J. Climatol.*, *15*, 1087–1097.

Brath, A., A. Montanari, and G. Moretti (2006), Assessing the effect on flood frequency of land use change via hydrological simulation (with uncertainty), *J. Hydrol.*, *324*, 141–153.

Cannon, A. J., and P. H. Whitfield (2002), Downscaling recent streamflow conditions in British Columbia, Canada using ensemble neural network models, *J. Hydrol.*, *259*, 136–151.

Dessai, S., X. Lu, and M. Hulme (2005), Limited sensitivity analysis of regional climate change probabilities for the 21st century, *J. Geophys. Res.*, *110*, D19108, doi:10.1029/2005JD005919.

Drakopoulos, J. A. (1995), Probabilities, possibilities, and fuzzy sets, *Fuzzy Sets Systems*, *75*(1), 1–15.

Dubois, D. (2006), Possibility theory and statistical reasoning, *Comput. Stat. Data Anal.*, *51*, 47–69.

Ghosh, S., and P. P. Mujumdar (2007a), Nonparametric methods for modeling GCM and scenario uncertainty in drought assessment, *Water Resour. Res.*, *43*, W07405, doi:10.1029/2006WR005351.

Ghosh, S., and P. P. Mujumdar (2007b), Modeling GCM and scenario uncertainty: an imprecise probability approach, 3rd Indian International Conference on Artificial Intelligence, Pune, India, December, 2007.

Ghosh, S., and P. P. Mujumdar (2008), Statistical downscaling of GCM simulations to streamflow using relevance vector machine, *Adv. Water Resour.*, *31*(1), 132–146, doi:10.1016/j.advwatres.2007.07.005.

Giorgi, F., and L. O. Mearns (2003), Probability of regional climate change calculated using the reliability ensemble averaging (REA) method, *Geophys. Res. Lett.*, *30*(12), 1629, doi:10.1029/2003GL017130.

Güler, C., and G. D. Thyne (2004), Delineation of hydrochemical facies distribution in a regional groundwater system by means of fuzzy c-means clustering, *Water Resour. Res.*, *40*, W12503, doi:10.1029/2004WR003299.

Hughes, J. P., and P. Guttorp (1994), A class of stochastic models for relating synoptic atmospheric patterns to regional hydrologic phenomena, *Water Resour. Res.*, *30*(5), 1535–1546.

Huth, R. (2004), Sensitivity of local daily temperature change estimates to the selection of downscaling models and predictors, *J. Clim.*, *17*, 640–651.

IPCC (2001), Climate Change 2001 – The Scientific Basis, Contribution of Working Group I to the Third Assessment Report of the Intergovernmental Panel on Climate Change, edited by J. T. Houghton et al., Cambridge Univ. Press, Cambridge, UK.

Jones, R. N. (2000), Analysing the risk of climate change using an irrigation demand model, *Clim. Res.*, *14*, 89–100.

Kalnay, E., et al. (1996), The NCEP/NCAR 40-year reanalysis project, *Bull. Am. Meteorol. Soc.*, *77*(3), 437–471.

Nash, J. E., and J. V. Sutcliffe (1970), River flow forecasting through conceptual models. Part-1: A discussion of principles, *J. Hydrol.*, *10*, 282–290.

New, M., and M. Hulme (2000), Representing uncertainty in climate change scenarios: A Monte Carlo approach, *Int. Assessment*, *1*, 203–213.

Rao, P. G., and K. K. Kumar (1992), Climatic shifts over Mahanadi river basin, *Curr. Sci.*, *63*, 192–196.

Rao, P. G. (1995), Effect of climate change on streamflows in the Mahanadi river basin, India, *Water Int.*, *20*, 205–212.

Ross, T. J. (1997), *Fuzzy Logic With Engineering Applications*, pp. 379–396, McGraw-Hill, New York.

Simonovic, S. P., and E. G. R. Davies (2006), Are we modelling impacts of climatic change properly?, *Hydrol. Processes*, *20*, 431–433.

Simonovic, S. P., and L. Li (2003), Methodology for assessment of climate change impacts on large-scale flood protection system, *J. Water Resour. Plann. Manage.*, *129*(5), 361–371.

Simonovic, S. P., and L. Li (2004), Sensitivity of the Red River Basin flood protection system to climate variability and change, *Water Resour. Manage.*, *18*, 89–110.

Spott, M. (1999), A theory of possibility distributions, *Fuzzy Sets Systems*, *102*(2), 135–155.

Tebaldi, C., L. O. Mearns, D. Nychka, and R. L. Smith (2004), Regional probabilities of precipitation change: A Bayesian analysis of multimodel simulations, *Geophys. Res. Lett.*, *31*, L24213, doi:10.1029/2004GL021276.

Tebaldi, C., R. Smith, D. Nychka, and L. O. Mearns (2005), Quantifying uncertainty in projections of regional climate change: A Bayesian approach to the analysis of multi-model ensembles, *J. Clim.*, *18*, 1524–1540.

Tipping, M. E. (2001), Sparse Bayesian learning and the relevance vector machine, *J. Mach. Learning Res.*, *1*, 211–244.

Tonn, B. (2005), Imprecise probabilities and scenarios, *Futures*, *37*, 767–775.

Tripathi, S., V. V. Srinivas, and R. S. Nanjundiah (2006), Downscaling of precipitation for climate change scenarios: A support vector machine approach, *J. Hydrol.*, *330*(3–4), 621–640.

Wetterhall, F., S. Halldin, and C. Xu (2005), Statistical precipitation downscaling in central Sweden with the analogue method, *J. Hydrol.*, *306*, 174–190.

Wilby, R. L., L. E. Hay, and G. H. Leavesly (1999), A comparison of downscaled and raw GCM output: Implications for climate change scenarios in the San Juan river basin, Colorado, *J. Hydrol.*, *225*, 67–91.

Wilby, R. L., and C. W. Dawson (2004), Using SDSM version 3.1, A decision support tool for the assessment of regional climate change impacts, user manual.

Wilby, R. L., S. P. Charles, E. Zorita, B. Timbal, P. Whetton, and L. O. Mearns (2004), The guidelines for use of climate scenarios developed from statistical downscaling methods, Supporting material of the Intergovernmental Panel on Climate Change (IPCC), prepared on behalf of Task Group on Data and Scenario Support for Impacts and Climate Analysis (TGICA) (available at http://ipccddc.cru.uea/ac.uk/guidelines/StatDownGuide.pdf).

Wilby, R. L., and I. Harris (2006), A framework for assessing uncertainties in climate change impacts: Low-flow scenarios for the River Thames, UK, *Water Resour. Res.*, *42*, W02419, doi:10.1029/2005WR004065.

Willmott, C. J., C. M. Rowe, and W. D. Philpot (1985), Small-scale climate map: A sensitivity analysis of some common assumptions associated with the grid-point interpolation and contouring, *Am. Cartogr.*, *12*, 5–16.

Wood, A. W., E. P. Maurer, A. Kumar, and D. P. Lettenmaier (2002), Long-range experimental hydrologic forecasting for the eastern United States, *J. Geophys. Res.*, *107*(D20), 4429, doi:10.1029/2001JD000659.

Zadeh, L. A. (1978), Fuzzy sets as a basis for a theory of possibility, *Fuzzy Sets Systems*, *1*(1), 3–28.

S. Ghosh, Department of Civil Engineering, Indian Institute of Technology Bombay, Powai, Mumbai 400 076, India. (subimal@civil.iitb.ac.in)

P. P. Mujumdar, Department of Civil Engineering, Indian Institute of Science, Bangalore 560 012, India. (pradeep@civil.iisc.ernet.in)